Check for updates

miR-423-5p and miR-92a-3p in Alzheimer's disease: relationship with pathology and cognition

Sang-Won Han[1], Young Ho Park[2]*, Jung-Min Pyun[2],
Paula J. Bice[3], SangYun Kim[2], Andrew J. Saykin[3] and
Kwangsik Nho[3]*

[1]Department of Neurology, Soonchunhyang University Seoul Hospital and Soonchunhyang University
College of Medicine, Seoul, Republic of Korea, [2]Department of Neurology, Seoul National University
Bundang Hospital and Seoul National University College of Medicine, Seongnam-si, Republic of
Korea, [3]Department of Radiology and Imaging Sciences, Center for Computational Biology and
Bioinformatics, Indiana Alzheimer's Disease Research Center, Indiana University School of Medicine,
Indianapolis, IN, United States

Background: MicroRNAs (miRNAs), small and highly conserved non-coding RNA molecules, have emerged as promising molecular biomarkers due to their regulatory roles in gene expression and stability in blood.

Methods: We used measurements of 64 plasma miRNAs from 145 participants in the Alzheimer's disease Neuroimaging Initiative cohort, including 74 probable AD patients and 71 cognitively normal (CN) older adults. We performed principal component analysis (PCA) with factor rotation for dimension reduction to identify AD-associated principal components (PCs) and their key miRNAs with factor loadings higher than 0.8. We investigated their association with amyloid/tau/neurodegeneration (A/T/N) biomarkers and cognition. After identifying the candidate target genes of key miRNAs, we performed pathway enrichment analysis. We conducted mediation analyses to assess the effect of the associations between miRNAs and A/T/N biomarkers on AD diagnosis and cognition. Finally, we used a machine learning approach to evaluate the performance of key miRNAs for AD classification.

Results: PCA identified one PC as significantly associated with AD. The PC was also significantly associated with CSF p-tau levels, hippocampal volume, and cognition. Two key miRNAs (miR-423-5p and miR-92a-3p) in the PC were associated with AD. Lower levels of miR-423-5p and miR-92a-3p were associated with reduced hippocampal volume and worse cognition, and lower levels of miR-423-5p were associated with higher brain amyloid deposition. Pathway enrichment analysis identified several significant biological processes, including memory, protein phosphorylation, and the phosphatidylinositol-3-phosphate biosynthetic process. Mediation analysis revealed that miR-423-5p, but not miR-92a-3p, had indirect effects on AD diagnosis and memory performance through brain amyloid deposition and brain atrophy. Machine learning analysis demonstrated that incorporating two key miRNAs improved the performance of demographic information for AD classification.

Conclusion: Plasma miR-423-5p and miR-92a-3p are implicated in AD pathology and cognitive decline, providing insights into their roles in disease mechanisms. This study suggests the potential of these miRNAs as blood-based molecular biomarkers for AD.

1 Introduction

Alzheimer's disease (AD) is a progressive neurodegenerative disorder that stands as a common cause of dementia among older adults (Long and Holtzman, 2019). AD manifests through a constellation of neuropathological features, including the extracellular accumulation of amyloid-β (Aβ) plaques along with intracellular neurofibrillary tangles (NFTs) composed of hyperphosphorylated tau protein aggregates (Long and Holtzman, 2019). Despite extensive research efforts, the pathogenesis of AD remains elusive, largely due to its complex neurochemical and genetic landscape (Hampel et al., 2010).

Significant advancements have been made in antemortem diagnosis of AD through the use of biomarkers obtained from cerebrospinal fluid (CSF) or visualized via positron emission tomography (PET) imaging (Long and Holtzman, 2019; Schindler et al., 2024). These biomarkers have proven to be highly effective in identifying the pathological hallmarks of the disease (Hampel et al., 2018; Long and Holtzman, 2019; Schindler et al., 2024). However, the invasive nature of CSF collection and the high costs of PET imaging pose significant limitations to their widespread application in routine clinical practice (Hampel et al., 2018; Schindler et al., 2024). Consequently, there is a critical need for the identification of more accessible and less invasive biomarkers, such as blood-based ones, for AD diagnosis.

In recent years, microRNAs (miRNAs), which are non-coding RNA molecules approximately 20–23 nucleotides long, have emerged as potential biomarkers for AD (Wang et al., 2019; Kou et al., 2020). These miRNAs are involved in AD pathogenesis, playing important roles in post-transcriptional gene expression regulation by binding the 3′-untranslated regions of messenger RNAs (mRNAs) (Bartel, 2004; Winter et al., 2009; Wang et al., 2019; Kou et al., 2020). Notably, alterations in the levels of specific miRNAs in peripheral blood have been reported in AD patients, suggesting their potential utility as non-invasive biomarkers for AD (Kou et al., 2020; Guévremont et al., 2022). Given the stability of miRNAs in circulation and their detectability in various biological fluids including plasma, they represent promising candidates for the development of blood-based diagnostic biomarkers for AD (Weber et al., 2010; Turchinovich et al., 2011).

A critical step in analyzing high-dimensional biological data, such as miRNA expression data, is dimension reduction. This step is essential for simplifying complex datasets to enhance data interpretability while retaining the biological significance of the data (Meng et al., 2016). Principal component analysis (PCA) is a widely utilized method for dimension reduction, enabling the identification of underlying patterns in data that may not be apparent in high-dimensional space (Ringnér, 2008; Meng et al., 2016). Through the application of PCA, essential features are extracted from an extensive set of miRNAs, which helps elucidate the specific roles of miRNAs in AD and deepens understanding of their dysregulated expression in the context of the disease (Ringnér, 2008; Jolliffe and Cadima, 2016; Meng et al., 2016).

In this study, we investigated the association of circulating miRNAs with central AD biomarkers and their potential as candidate blood-based molecular biomarkers for AD using expression data from 64 individually measured plasma miRNAs from 145 participants in the Alzheimer's Disease Neuroimaging Initiative (ADNI) dataset. We performed PCA to identify AD-associated principal components (PCs) and their key miRNAs. Subsequently, we also investigated their association with amyloid/tau/neurodegeneration (A/T/N) biomarkers and cognitive function, aiming to contribute to the identification of potential blood-based molecular biomarkers for AD. After identifying the candidate target genes of these miRNAs, we investigated their involvement in biological pathways to provide insights into the molecular mechanisms underpinning AD. Furthermore, we performed mediation analysis to assess the effect of the associations between miRNAs and A/T/N biomarkers on AD diagnosis and cognitive function. Finally, we conducted a machine learning approach to evaluate the performance of miRNAs for the classification of AD.

2 Materials and methods

2.1 Study samples

The ADNI was launched in 2003 through a collaborative effort including the National Institute on Aging, National Institute of Biomedical Imaging and Bioengineering, Food and Drug Administration, private pharmaceutical companies, and nonprofit organizations. The initial phase, ADNI-1 (Petersen et al., 2010), aimed to assess the feasibility of using serial magnetic resonance imaging (MRI), PET scans, various biological markers, and clinical and neuropsychological assessments as reliable indicators of AD pathogenesis. This was followed by subsequent phases—ADNI-GO (Aisen et al., 2010), ADNI-2 (Aisen et al., 2015), and ADNI-3 (Weiner et al., 2017)—which expanded on the initial phase by allowing for the continuous follow-up of existing participants and incorporating new enrollments. Detailed information on ADNI, including latest updates, eligibility criteria, protocols for clinical and neuroimaging evaluations, and an outline of diagnostic criteria is available at https://www.adni-info.org. The ADNI Laboratory of Neuro Imaging (LONI) website[1] provided access to demographic and clinical information, raw neuroimaging data, CSF biomarker data, apolipoprotein E (*APOE*) ε4 genotyping, and cognitive scores. All participants provided written informed consent at the time of enrollment, which included consent for data analysis and sharing. The study received approval from the Institutional Review Board at each participating site. Participants diagnosed with probable AD and cognitively normal (CN) were followed up prospectively with clinical data, neuroimaging studies, and biological samples for molecular biomarker measurements, as

---

1   http://adni.loni.usc.edu

previously described (Aisen et al., 2010; Petersen et al., 2010; Aisen et al., 2015; Weiner et al., 2017). Diagnostic classifications were based on assessments including the Logical Memory from the Wechsler Memory Scale—Revised (Wechsler, 1987), Mini-Mental State Examination (MMSE) (Folstein et al., 1975), and Clinical Dementia Rating scale (Morris, 1993).

2.2 miRNA expression data

To assess concordance of miRNA expression between CSF and plasma, the same RT-qPCR workflow was applied to both biofluids using a custom TaqMan Advanced Human miRNA Low-Density Array (TLDA) card containing 64 preselected miRNAs. These miRNAs were selected based on prior literature demonstrating their detectability in CSF (Lusardi et al., 2016; Saugstad et al., 2017; Wiedrick et al., 2019; Sandau et al., 2020b; Sandau et al., 2022) and plasma (Sandau et al., 2020a) and their established relevance to AD. RNA isolation was conducted in 24-sample batches, including matched CSF and plasma samples to mitigate batch effects. Total RNA was extracted from 250 μL each of CSF and plasma using the miRNA Purification kit, following the manufacturer's protocol (Abdalla et al., 2011). A 3 pM concentration of the exogenous spike-in cel-miR-39-3p was added following the lysis step. RNA elution was performed with 30 μL of nuclease-free water for CSF samples and 50 μL for plasma samples. Quantification of miRNA was performed using the Qubit miRNA Assay kit and Qubit 4.0 fluorometer (Scientific, 2017). For reverse transcription quantitative polymerase chain reaction, miRNA was reverse transcribed to complementary DNA (cDNA) using the TaqMan Advanced miRNA cDNA Synthesis kit according to the manufacturer's instructions (TaqMan, 2011). This process included poly-adenylation and adaptor ligation, followed by reverse transcription, and a universal 14-cycle miRNA amplification. The diluted miRNA amplification reaction mixture was combined with TaqMan Fast Advanced master mix and then loaded onto a custom TLDA card for assay on a QuantStudio 7 Flex. Data analysis included a detailed examination of quantification cycle (Cq) values for artifacts and quality control (QC) using array card well-level statistics. For both CSF and plasma samples, Cq values were normalized using the exogenous spike-in control cel-miR-39-3p and the endogenous reference hsa-miR-16-5p (Moldovan et al., 2014). Handling of censored values (Cq > 34) was performed through censoring-aware methods, as previously described in detail (Wiedrick et al., 2019; Sandau et al., 2024).

All 64 miRNAs passed predefined QC thresholds and were retained for downstream analysis. A total of 64 miRNAs were analyzed from 80 probable AD patients and 80 CN individuals. Participants who lacked one or more miRNA expression data were excluded for subsequent PCA, resulting in 74 probable AD patients and 71 CN individuals included for further analysis.

2.3 Neuroimaging data

Brain MRI scans were obtained from participants using 3 T scanners, following the ADNI standardized protocol for 3D Magnetization Prepared Rapid Gradient Echo sequences. The scans were processed through the longitudinal pipeline of FreeSurfer version 5.3, as previously described (Jack et al., 2008; Jack et al., 2010),

enabling the extraction of critical regions of interest, such as the bilateral hippocampal volumes and total intracranial volume.

Additionally, preprocessed [18F] florbetapir PET scans were sourced from the ADNI database via the LONI platform (see text footnote 1, respectively) and were acquired in line with the protocols established by previous studies (Jagust et al., 2010; Jagust et al., 2015). The quantification of amyloid burden was conducted by analyzing the standard uptake value ratio (SUVR) values from [18F] florbetapir PET scans, which is essential for evaluating amyloid deposits in the brain. These SUVR values were normalized to the intensity measurements from the cerebellum, which served as a reliable reference region (Joshi et al., 2012). To correct for skewness in the distribution of florbetapir PET SUVR data, a logarithmic transformation was applied.

2.4 CSF biomarkers

CSF samples were collected through lumbar puncture in the morning, following an overnight fast. These samples were frozen within 1 h of collection and transported to the ADNI Biomarker Core Laboratory at the University of Pennsylvania Medical Center, according to the ADNI protocol (Kang et al., 2015). Concentrations of Aβ42 and phosphorylated tau181 (p-tau) in CSF were measured using the Roche Elecsys Aβ42 and p-tau CSF immunoassays, respectively, as previously outlined (Bittner et al., 2016; Hansson et al., 2018). The CSF biomarker data were accessed and downloaded from the ADNI LONI website (see text footnote 1, respectively). To correct for data skewness, a logarithmic transformation of the CSF biomarker data was performed.

2.5 Comprehensive neuropsychological assessment

Domain-specific cognitive composite scores were calculated for memory and executive function. The composite score for memory integrated results from the Alzheimer's Disease Assessment Scale-Cognitive Subscale (Mohs et al., 1997), the Rey Auditory Verbal Learning Test (Rey, 1983), the memory components of the MMSE (Folstein et al., 1975), and the Logical Memory task (Wechsler, 1987). For executive function, the composite score included assessments from the Wechsler Adult Intelligence Scale–Revised Digit Symbol Substitution task (Wechsler and De Lemos, 1981) and the Digit Span backward task (Wechsler, 1987), the Trail Making Test Parts A and B (Reitan and Wolfson, 1985), category fluency (animals and vegetables) (Morris et al., 1989), and five clock drawing tasks. To ensure comparability and consistency across individuals within the ADNI cohorts, these composite scores were standardized to a mean value of 0 and a standard deviation of 1.

2.6 A/T/N biomarkers

We used CSF Aβ42 levels and global cortical amyloid deposition measured from amyloid PET scans as biomarkers of Aβ (A), CSF p-tau levels as a biomarker of tau (T), and structural hippocampal atrophy on brain MRI as a biomarker of neurodegeneration (N), as described in the National Institute on Aging–Alzheimer's Association Research Framework (Jack et al., 2024).

2.7 Dimension reduction in miRNA expression analysis using PCA

The procedure for PCA commenced with the extraction of PCs followed by an orthogonal rotation to maximize the variance explained by each PC, thus streamlining the data structure while preserving critical biological information (Jolliffe, 2002; Ringnér, 2008). The selection process for PCs was based on rigorous criteria, only retaining components with eigenvalues over 1. This threshold is widely accepted for ensuring the inclusion of PCs representing significant variance and relevance (Jolliffe, 2002; Peres-Neto et al., 2005). A factor loading threshold exceeding 0.8 was applied to identify the key miRNAs for each rotated PC, thereby focusing exclusively on miRNAs that have a substantial impact on the PCs. This selective approach aligns with methodologies that aim to improve data interpretability and significance (Fabrigar et al., 1999), excluding miRNAs with lower loadings from further analysis.

2.8 Identification of target genes for key miRNAs in AD-associated PCs

To understand the biological implications of the key miRNAs identified in the PCs associated with AD, their target genes were predicted using two well-known databases: TargetScan (Lewis et al., 2005) and miRDB (Wong and Wang, 2015). These databases are pivotal in the field of miRNA research, offering a comprehensive collection of both predicted and experimentally validated interactions that outline the relationships between miRNAs and their corresponding target genes. To ensure the robustness of our analysis, we applied a rigorous selection criterion for further analysis, focusing only on target genes consistently identified in both databases.

2.9 Pathway-based enrichment analysis of target genes

To explore intricate molecular pathways and biological processes implicated by the target genes of AD-associated key miRNAs, a gene-set enrichment analysis was performed using the Database for Annotation, Visualization, and Integrated Discovery (DAVID) online resource (Huang et al., 2009). DAVID is widely recognized for its comprehensive analytical framework, enabling the systematic identification of functionally related gene groups and their associated biological pathways. We specifically focused on the Gene Ontology (GO) - particularly the Biological Processes (BP) category (Ashburner et al., 2000). To adjust for multiple testing, Bonferroni correction (Dunn, 1961) was applied by dividing the significance threshold by the number of GO-BP terms tested within this specific category.

2.10 Statistical analysis

For the PCs of miRNAs, logistic regression models were used to evaluate the association of the PCs and key miRNAs with AD diagnosis to identify the AD-associated PCs and key miRNAs.

Linear regression models were used to assess the association of the AD-associated PCs and key miRNAs with global cortical amyloid deposition, hippocampal volume, and CSF biomarkers for AD, including Aβ42 and p-tau. Moreover, linear regression models were used to investigate the association of the AD-associated PCs and key miRNAs with baseline composite scores for memory and executive function, while linear mixed effects models were used to evaluate their association with longitudinal changes in the composite scores of memory and executive function. In all association analyses, age and sex were consistently included as covariates. Additional covariates included years of education for cognitive performance, *APOE* ε4 carrier status for global cortical amyloid deposition, CSF Aβ42, and CSF p-tau, and intracranial volume for hippocampal volume. For the association analysis of PCs with AD diagnosis, the false discovery rate (FDR) correction with the Benjamini-Hochberg procedure was used to adjust for multiple testing (Benjamini and Hochberg, 1995).

To assess the potential modifying effects of sex on the associations between miRNAs and A/T/N biomarkers, we conducted stratified linear regression analyses separately in males and females. The stratification variable sex was not included as a covariate in the sex-stratified analyses. Covariate-adjusted regression coefficients were transformed into sample size-weighted standardized effect sizes (Cohen's d) to formally compare the strength of associations between subgroups (Paternoster et al., 1998). A two-sided p-value was calculated from the t-statistic using a standard normal distribution to assess sex-specific differences in A/T/N biomarkers based on standardized effect sizes. Additionally, we quantified the magnitude of effect heterogeneity between subgroups using the I^2 statistic (Higgins and Thompson, 2002). An I^2 value above 50% was considered indicative of substantial heterogeneity. To complement the subgroup difference analyses, we also included an interaction term between sex and miRNA in the pooled linear regression model. The p value for the interaction term was calculated to evaluate whether the association between each miRNA and A/T/N biomarkers significantly differed between male and female subgroups. In accordance with previously established methodology (Arnold et al., 2020), we classified miRNA-A/T/N biomarker associations into homogeneous effects if miRNAs showed very similar effects in their association to the biomarker for both sexes (i.e., estimated heterogeneity $p > 0.05$), and heterogeneous effects if miRNAs showed different effects in both sexes leading to significant heterogeneity (i.e., estimated heterogeneity $p < 0.05$) and/or the interaction between sex and miRNA. Effects that were significant in only one sex with either significant effect heterogeneity between males and females or significant interaction between sex and miRNA were considered sex-specific.

For the key miRNAs, we performed Pearson correlation analyses of their expression levels between plasma and CSF in participants with paired biofluid samples.

We performed mediation analysis on the key miRNAs demonstrating a significant correlation with AD diagnosis and a composite score of memory, following established methodologies (Hayes, 2009). Our investigation aimed to determine whether the identified relationships could be mediated by biomarkers for AD. For these analyses, we used the Mediation R package, which
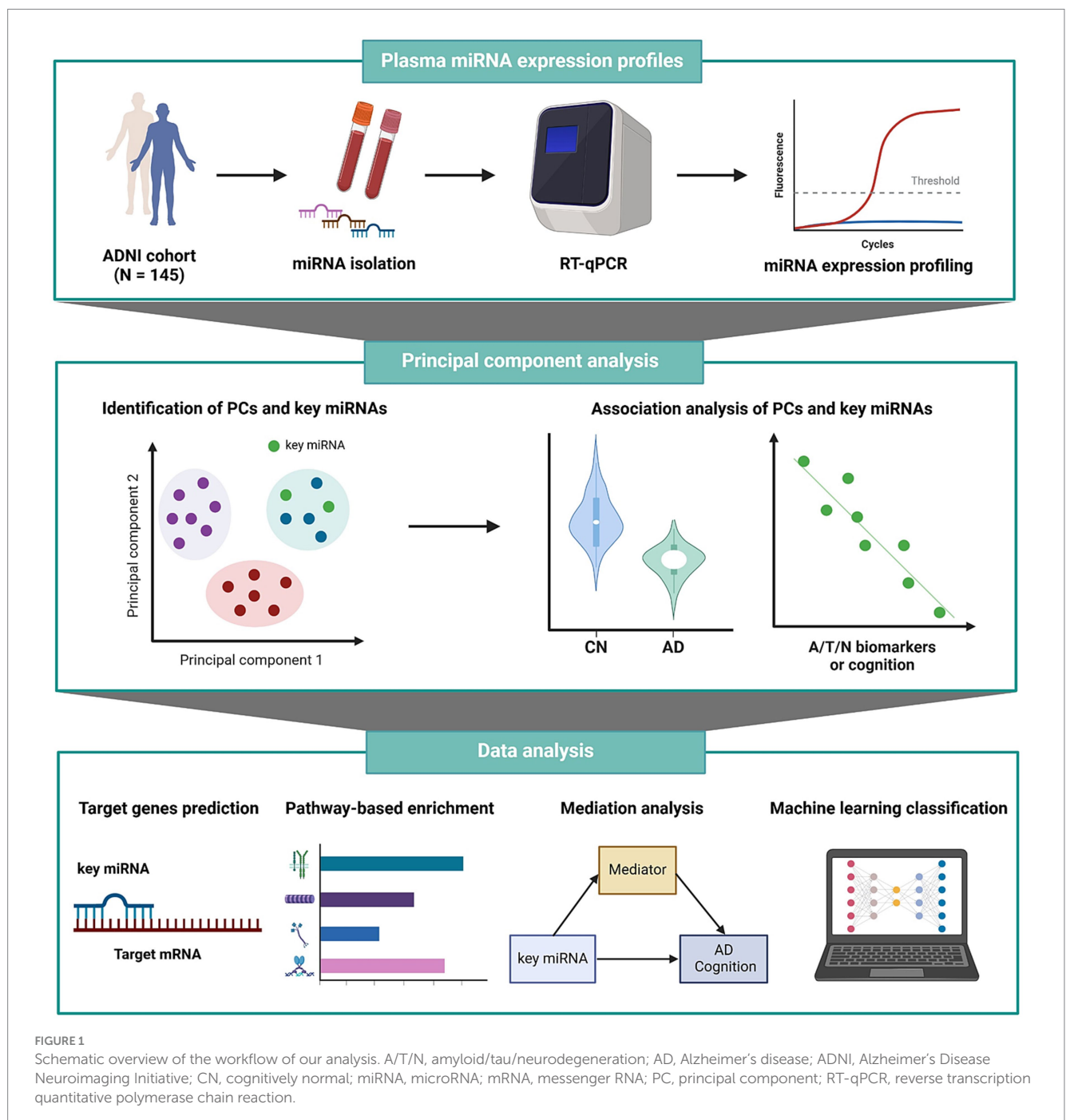
allowed for the evaluation of indirect effects through a bootstrapping approach (Tingley et al., 2014).

To investigate the classification performance of AD-associated key miRNAs in distinguishing AD patients from CN individuals, we applied the STREAMLINE tool (Urbanowicz et al., 2023), using an extreme gradient boosting machine learning approach. This machine learning approach is selected for integrating multi-view biological data and heterogeneous feature sets for the analysis of complex biological systems (Li et al., 2018). The dataset was randomly partitioned into 70% for training the model and 30% for testing, with a 5-fold cross-validation process to enhance the robustness and reliability of model evaluation. The classification performance of two different models in differentiating AD from CN was assessed through the receiver operating characteristic (ROC) curve and the area under the receiver operating characteristic curve (AUC). In terms of feature selection, Model 1 included age, sex, and *APOE* ε4 carrier status, while Model 2 incorporated all features from Model 1 and additionally included AD-associated key miRNAs, aiming to investigate their additional classification performance values in distinguishing AD from CN.

All statistical analyses were performed using R software, version 4.2.2. We defined statistical significance at a p value threshold of less than 0.05, incorporating adjustments for multiple comparisons. The workflow of all analysis steps used in this study is shown in Figure 1.

FIGURE 1
Schematic overview of the workflow of our analysis. A/T/N, amyloid/tau/neurodegeneration; AD, Alzheimer's disease; ADNI, Alzheimer's Disease Neuroimaging Initiative; CN, cognitively normal; miRNA, microRNA; mRNA, messenger RNA; PC, principal component; RT-qPCR, reverse transcription quantitative polymerase chain reaction.

3 Results

3.1 Demographic and clinical characteristics

We used miRNA expression data from 145 ADNI participants, including 74 probable AD patients and 71 CN individuals, as detailed in Table 1. The median age was 74.5 years, with 56.3% being females. No significant differences were observed in sex distribution and age across the diagnostic groups. However, a substantial difference in *APOE* ε4 carrier status was noted, with a higher prevalence in AD patients compared to CN individuals. For the A/T/N biomarkers, CSF Aβ42 and hippocampal volume were significantly lower, and CSF p-tau levels and global cortical amyloid deposition were significantly higher in AD patients compared to CN individuals. Furthermore, composite scores for memory and executive function were significantly lower in AD patients compared to CN individuals.

3.2 Principal component analysis for dimension reduction of miRNA expression data

PCA was performed on 64 miRNAs in 74 probable AD patients and 71 CN individuals from the ADNI cohort. Dimension reduction with PCA resulted in 13 PCs with eigenvalues > 1 (Supplementary Table S1). After selecting key miRNAs with a factor loading ≥ 0.8 in each principal component, 7 of 13 PCs remained for further analysis (Supplementary Table S2).

Association analysis of the 7 PCs with AD diagnosis identified PC2 as significantly associated with AD after multiple comparison correction (odds ratio (OR) = 0.59, FDR-corrected p = 0.038; Figure 2; Supplementary Table S3).

3.3 Association of AD-associated PC2 with A/T/N biomarkers

The PC2 was investigated to assess its associations with central A/T/N biomarkers for AD. Lower PC2 scores were significantly associated with higher levels of CSF p-tau (β = −0.035 ± 0.016, p = 0.033) and reduced hippocampal volume (β = 90.105 ± 39.647, p = 0.025; Figures 3A,B; Supplementary Table S4).

FIGURE 2
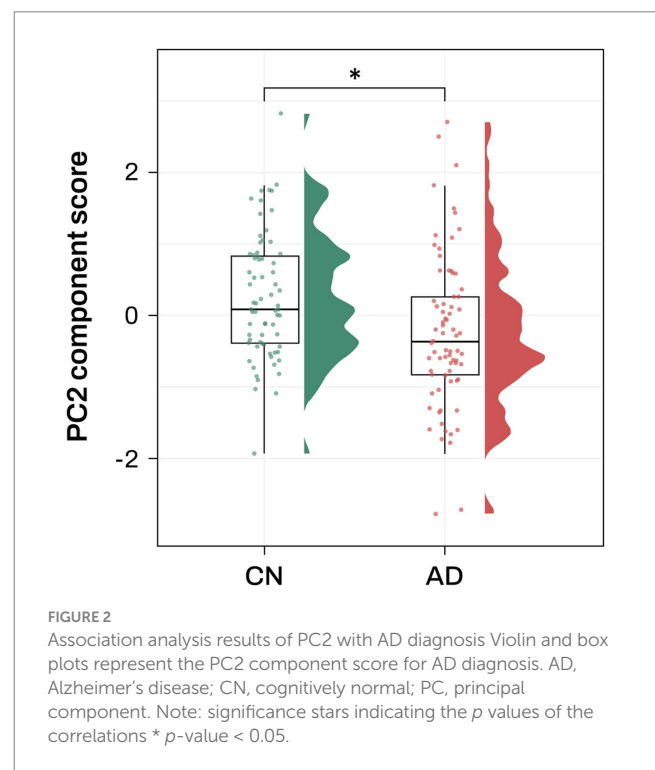Association analysis results of PC2 with AD diagnosis Violin and box plots represent the PC2 component score for AD diagnosis. AD, Alzheimer's disease; CN, cognitively normal; PC, principal component. Note: significance stars indicating the p values of the correlations * p-value < 0.05.

TABLE 1 Demographic information of participants from the ADNI cohort.

	CN (*n* = 71)	AD (*n* = 74)	Total (*n* = 145)	*p* value[b]
Male (%)	36 (50.7)	44 (59.5)	80 (55.2)	0.289
Age, years[a]	73.7 (69.7–78.8)	75.7 (69.1–80.7)	74.5 (69.6–79.7)	0.335
Education, years[a]	16 (14–18)	16 (13–16)	16 (14–18)	0.011
APOE ε4 carrier (%)	21 (29.6)	50 (67.6)	71 (49.0)	<0.001
CSF Aβ42, pg/mL[a]	1255.5 (826.5–1800.5)	650.2 (482.7–814.0)	809.7 (577.6–1411.0)	<0.001
CSF p-tau, pg/mL[a]	19.2 (16.7–24.2)	33.6 (27.4–47.5)	26.5 (18.7–36.7)	<0.001
Amyloid PET global SUVR[a]	1.04 (0.98–1.19)	1.46 (1.32–1.58)	1.24 (1.03–1.47)	<0.001
Hippocampal volume, mm[3a]	3,753 (3,520 – 4,000)	3,020 (2,794 – 3,266)	3,385 (2,974 – 3,777)	<0.001
Intracranial volume, mm[3a]	1,481,766 (1,366,350 – 1,633,833)	1,458,122 (1,371,248 – 1,592,867)	1,469,878 (1,369,858 – 1,629,653)	0.899
Baseline memory, Z scores[a]	0.93 (0.56–1.23)	−0.75 (−1.00 – −0.58)	−0.07 (−0.75–0.88)	<0.001
Baseline executive function, Z scores[a]	0.68 (0.42–1.07)	−0.39 (−0.97–0.07)	0.24 (−0.46–0.73)	<0.001

Values are *n* (%), unless indicated otherwise. [a]Data are presented as median followed by (interquartile range). [b]The Mann–Whitney U test or chi-square test was used to determine the p value for comparisons between AD and CN groups, as appropriate. Aβ, amyloid-β; AD, Alzheimer's disease; ADNI, Alzheimer's Disease Neuroimaging Initiative; APOE, apolipoprotein E; CN, cognitively normal; CSF, cerebrospinal fluid; p-tau, phosphorylated tau; PET, positron emission tomography; SUVR, standard uptake value ratio.
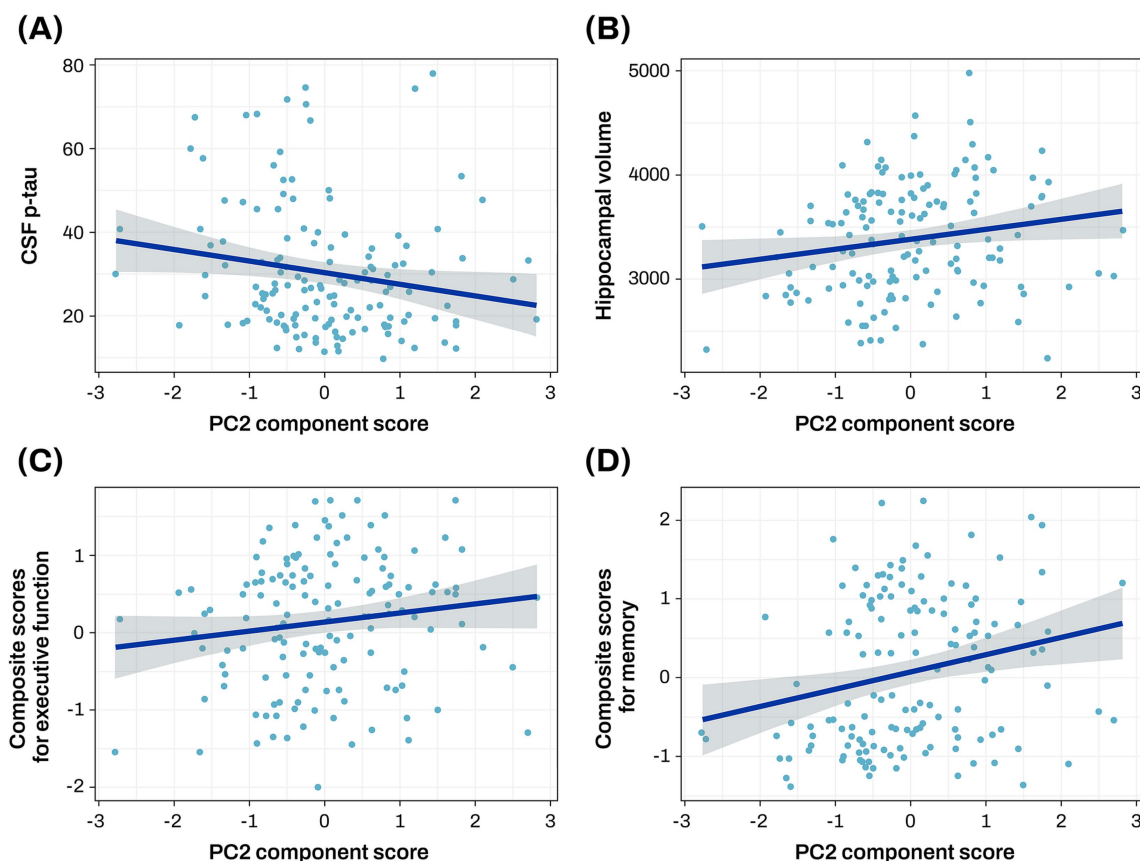
FIGURE 3
Association analysis results of PC2 with CSF p-tau, hippocampal volume, and cognitive function The scatter plot represents a correlation of the PC2 component score with CSF p-tau **(A)**, hippocampal volume **(B)**, baseline composite score for executive function **(C)**, and baseline composite score for memory **(D)**. The gray zone around the linear regression line represents the 95% confidence interval. Hippocampal volume was measured in cubic millimeters (mm^3). CSF biomarker concentrations were log-transformed and reported in picograms per milliliter (pg/mL). Cognitive scores were standardized as Z-scores. AD, Alzheimer's disease; CN, cognitively normal; CSF, cerebrospinal fluid; p-tau, phosphorylated tau; PC, principal component.

3.4 Association of AD-associated PC2 with cognition at baseline and longitudinal change of cognition

The PC2 was investigated to assess its associations with composite scores for memory and executive function at baseline and longitudinal changes of composite scores for memory and executive function. Higher PC2 scores were associated with better baseline composite scores for memory ($\beta = 0.222 \pm 0.074$, $p = 0.003$) and executive function ($\beta = 0.135 \pm 0.064$, $p = 0.038$; Figures 3C,D; Supplementary Table S5), and slower longitudinal decline of composite scores for memory ($\beta = 0.234 \pm 0.086$, $p = 0.008$; Figure 4; Supplementary Table S5).

3.5 Association of key miRNAs in the AD-associated PC2 with AD diagnosis and A/T/N biomarkers

In the AD-associated PC2, two miRNAs, miR-423-5p and miR-92a-3p, with a factor loading higher than 0.8 were identified as key miRNAs (Supplementary Table S2). Further analyses were performed to investigate the association of these two key miRNAs with AD diagnosis and A/T/N biomarkers for AD. Expression levels of miR-423-5p and miR-92a-3p were significantly lower in AD patients

compared to CN individuals (miR-423-5p, $\beta = -44.438 \pm 15.286$, $p = 0.004$; miR-92a-3p, $\beta = -41.606 \pm 13.018$, $p = 0.001$; Figures 5A,B). Lower expression levels of miR-423-5p and miR-92a-3p were significantly associated with reduced hippocampal volume (miR-423-5p, $\beta = 8.162 \times 10^3 \pm 3.279 \times 10^3$, $p = 0.014$; miR-92a-3p, $\beta = 6.366 \times 10^3 \pm 2.632 \times 10^3$, $p = 0.017$), and lower expression levels of miR-423-5p were associated with higher global cortical amyloid deposition ($\beta = -1.118 \pm 0.561$, $p = 0.048$; Figures 5C, 6A).

We conducted sex-stratified association analyses and subsequently assessed heterogeneity in effect estimates between males and females. Figure 6 details the results of miRNA associations with A/T/N biomarkers, including sex-by-miRNA interaction analyses. We identified a significant homogeneous association between miR-423-5p and global cortical amyloid deposition. In contrast, both miR-423-5p and miR-92a-3p exhibited male-specific associations with reduced hippocampal volume.

3.6 Association of key miRNAs in the AD-associated PC2 with cognition at baseline and longitudinal change of cognition

The two key miRNAs, miR-423-5p and miR-92a-3p, were investigated to assess their associations with composite scores for memory and executive function at baseline and longitudinal changes of composite
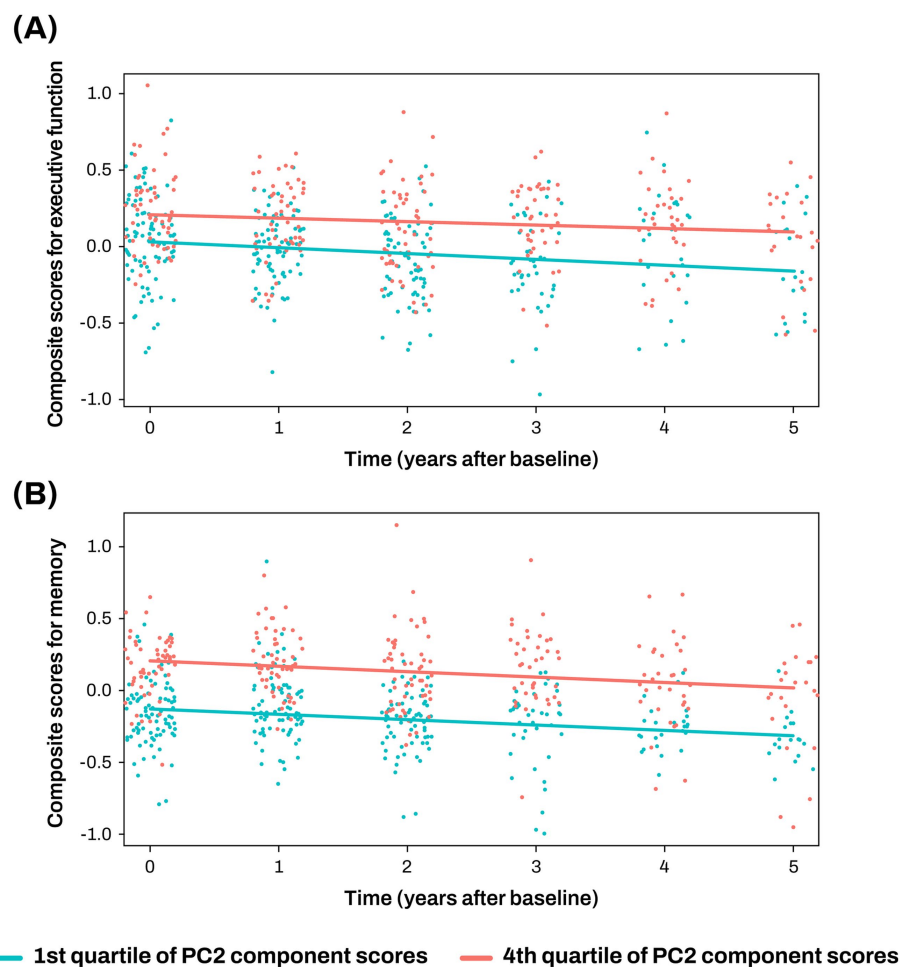
FIGURE 4
Association analysis results of PC2 with longitudinal changes of cognition **(A, B)** The x-axis represents years after the initial clinical evaluation, while the y-axis indicates composite scores for executive function **(A)** and memory **(B)**. The two lines represent the different slopes of changes in composite scores for subjects with 1st quartile (green color) versus 4th quartile (red color) stratified by PC2 component score. Cognitive scores were standardized as Z-scores. PC, principal component.

scores for memory and executive function. Higher expression levels of miR-423-5p and miR-92a-3p were significantly associated with better baseline composite scores for memory (miR-423-5p, $\beta = 20.164 \pm 6.098$, $p = 0.001$; miR-92a-3p, $\beta = 13.652 \pm 4.941$, $p = 0.006$) and executive function (miR-423-5p, $\beta = 13.348 \pm 5.317$, $p = 0.013$; miR-92a-3p, $\beta = 9.624 \pm 4.280$, $p = 0.026$; Figure 5C; Supplementary Table S6). Higher expression levels of miR-423-5p and miR-92a-3p were also significantly associated with slower longitudinal decline of composite scores for memory (miR-423-5p, $\beta = 21.573 \pm 7.133$, $p = 0.003$; miR-92a-3p, $\beta = 15.684 \pm 5.775$, $p = 0.007$), and lower expression levels of miR-423-5p were associated with slower longitudinal decline of composite scores for executive function ($\beta = 12.483 \pm 5.927$, $p = 0.037$; Figures 5C, 7; Supplementary Table S6).

3.7 Correlation between miRNA expression in plasma and CSF

The two key miRNAs, miR-423-5p and miR-92a-3p, were further investigated to evaluate their correlation between plasma and CSF

samples. The correlation analysis between plasma and CSF expression levels of miR-423-5p showed a significant correlation ($r = 0.236$, $p = 0.004$), while the significant correlation was not observed with miR-92a-3p (Figure 8).

3.8 Predicted target genes for two key miRNAs and their pathway enrichment analysis

Target genes for the two miRNAs, miR-423-5p and miR-92a-3p, were obtained from the miRDB and TargetScan databases, resulting in 700 and 985 genes from the miRDB database, and 232 and 1,041 genes from the TargetScan database, respectively. 106 and 701 overlapping target genes for miR-423-5p and miR-92a-3p were then identified between the two databases (Supplementary Additional file). The GO analysis of the target genes for miR-423-5p and miR-92a-3p revealed significant enrichment in BP pathway related to positive regulation of transcription from RNA polymerase II promoter, negative
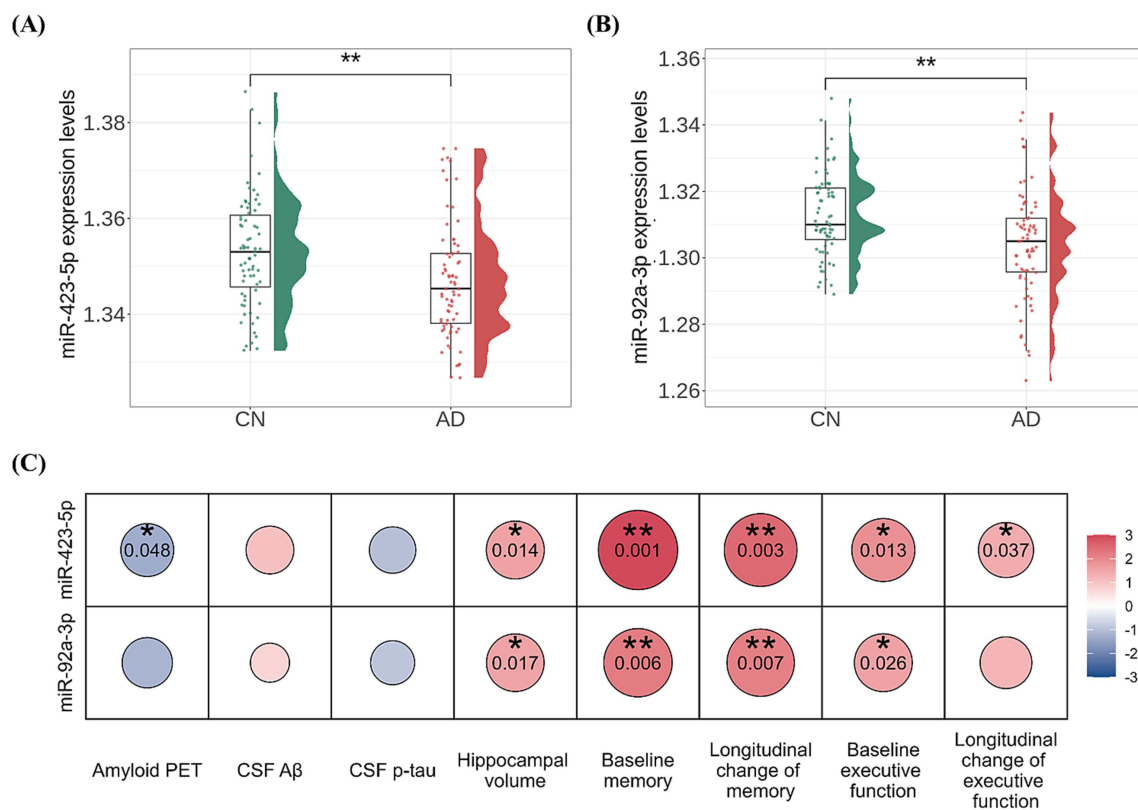
FIGURE 5
Association analysis results of miR-423-5p and miR-92a-3p with amyloid, tau, and neurodegeneration (A/T/N) biomarkers as well as cognition **(A, B)** Violin and box plots represent the miR-423-5p **(A)** and miR-92a-3p expression levels **(B)** for AD diagnosis **(C)**. Heatmap of association of miR-423-5p and miR-92a-3p expression levels with the "A/T/N" biomarkers for AD and cognition. p values were estimated from linear regression analyses. Circle color indicates the direction of the regression coefficient (β), while circle size and color intensity reflect the significance level of the association, quantified as $-\log$ (p value). The color bar represents $-\log$ (p value) $\times$ Sign(β). Red colors represent positive associations, and blue colors denote negative associations. The darker the color and larger the circle, the stronger the association. Hippocampal volume was measured in cubic millimeters (mm³). CSF biomarker concentrations were log-transformed and reported in picograms per milliliter (pg/mL). Cognitive scores were standardized as Z-scores. Aβ, amyloid-β; AD, Alzheimer's disease; CN, cognitively normal; CSF, cerebrospinal fluid; miR, microRNA; p-tau, phosphorylated tau; PET, positron emission tomography. Note: significance stars indicating the p values of the correlations adjustment for multiple comparisons * p-value < 0.05. ** p-value < 0.01.

regulation of transcription from RNA polymerase II promoter, brain development, protein phosphorylation, intracellular signal transduction, negative regulation of transcription, peptidyl-serine phosphorylation, nervous system development, neuron migration, memory, palate development, negative regulation of cytoplasmic translation, ventricular septum morphogenesis, cell migration, peptidyl-threonine phosphorylation, positive regulation of transcription, regulation of transcription from RNA polymerase II promoter, phosphatidylinositol-3-phosphate biosynthetic process, and cellular response to amino acid stimulus (Table 2).

3.9 Mediation analysis of two key miRNAs on AD or composite scores for memory

Mediation analysis revealed that miR-423-5p expression levels had both direct and indirect effects on AD through global cortical amyloid deposition (direct effect: $\beta = -2.61 \times 10^{-10}$; $p = 0.04$; indirect effect: $\beta = -2.61 \times 10^{-10}$; $p = 0.02$), while miR-423-5p expression levels had only indirect effects on AD

through hippocampal volume (direct effect: $\beta = -9.86 \times 10^{-16}$; $p = 0.16$; indirect effect: $\beta = -9.86 \times 10^{-16}$; $p = 0.02$; Figure 9; Supplementary Table S7). Additionally, miR-423-5p expression levels were found to affect composite scores for memory through both direct and indirect effects mediated by global cortical amyloid deposition (direct effect: $\beta = 10.29$; $p = 0.02$; indirect effect: $\beta = 4.44$; $p = 0.04$) and hippocampal volume (direct effect: $\beta = 8.52$; $p = 0.02$; indirect effect: $\beta = 7.80$; $p = 0.02$) (Figure 9; Supplementary Table S7). However, miR-92a-3p expression levels had no indirect effects on AD or composite scores for memory through hippocampal volume (Supplementary Table S7).

3.10 Machine learning analysis for AD classification

A machine learning approach, extreme gradient boosting, for the classification of AD patients from CN individuals was used to evaluate two different classification models. Results of the 5-fold cross-validation are presented in Figure 10. Model 1, including age, sex, and *APOE* ε4 carrier status, achieved a mean AUC value of 0.708. The

(A)
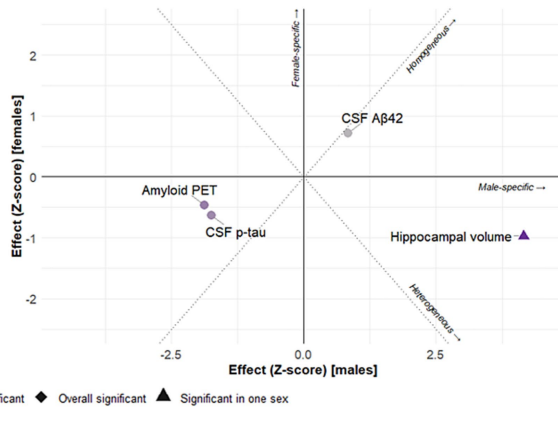
	miR-423-5p												
	Pooled analysis			Males (N = 80)			Females (N = 65)			Sex difference			Interaction	
Biomarkers	β	SE	P value	β	SE	P value	β	SE	P value	t	P value	I²	P value	Effect type
Amyloid PET global SUVR	-1.12	0.56	0.048	-1.79	0.688	0.011	0.04	0.94	0.967	-1.57	0.117	36.27	0.198	Homogenous
CSF Aβ42	2.89	1.66	0.085	3.75	2.149	0.085	0.85	2.64	0.747	0.85	0.395	0.00	0.359	Not significant
CSF p-tau	-2.28	1.37	0.098	-4.09	1.643	0.015	-0.12	2.31	0.957	-1.40	0.162	28.42	0.200	Not significant
Hippocampal volume	8.16E+03	3.28E+03	0.014	1.65E+04	4.10E+03	1.40E-04	-4.17E+03	5.02E+03	0.410	3.18	0.001	68.59	0.004	Male-specific

	miR-92a-3p												
	Pooled analysis			Males (N = 80)			Females (N = 65)			Sex difference			Interaction	
Biomarkers	β	SE	P value	β	SE	P value	β	SE	P value	t	P value	I²	P value	Effect type
Amyloid PET global SUVR	-0.86	0.46	0.065	-1.07	0.57	0.065	-0.36	0.78	0.645	-0.73	0.467	0.00	0.751	Not significant
CSF Aβ42	1.75	1.35	0.196	1.48	1.77	0.406	1.51	2.11	0.476	-0.01	0.990	0.00	0.999	Not significant
CSF p-tau	-1.71	1.11	0.124	-2.37	1.36	0.085	-1.17	1.85	0.531	-0.52	0.602	0.00	0.751	Not significant
Hippocampal volume	6.37E+03	2.63E+03	0.017	1.36E+04	3.26E+03	8.54E-05	-3.89E+03	4.01E+03	0.336	3.38	0.001	70.37	0.004	Male-specific
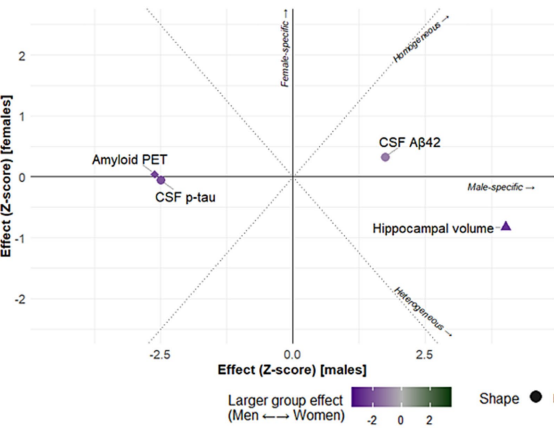
(B)   **(C)**

FIGURE 6
Association analysis results and sex-based effect heterogeneity of miR-423-5p and miR-92a-3p with amyloid, tau, and neurodegeneration (A/T/N) biomarkers **(A)** Linear regression results examining the associations between miRNAs and A/T/N biomarkers are presented for the full sample and stratified by sex, along with estimates of effect heterogeneity and *p* value for sex-by-miRNA interaction terms. Scatter plots display Z-scores of effect estimates for the associations of the miR-423-5p **(B)** and miR-92a-3p **(C)** with A/T/N biomarkers in males (x-axis) and females (y-axis). Homogeneous effects, defined as associations with comparable effect size in both sexes, appear along the diagonal. Heterogeneous effects appear along the anti-diagonal. Sex-specific effects are located near the x-axis (male-specific) or y-axis (female-specific effects). Homogeneous and overall significant results are indicated by diamonds, while effects significant in only one sex are represented as triangles. Sex-specific effects are further visualized using a color scale (purple for males; green for females). Hippocampal volume was measured in cubic millimeters (mm³). CSF biomarker concentrations were log-transformed and reported in picograms per milliliter (pg/mL). Aβ, amyloid-β; CSF, cerebrospinal fluid; miR, microRNA; p-tau, phosphorylated tau; PET, positron emission tomography; SE, Standard Error; SUVR, standardized uptake value ratio.

mean AUC value of Model 2, obtained by adding two AD-associated key miRNAs, miR-423-5p and miR-92a-3p, to Model 1, increased to 0.757.

4 Discussion

This study highlights the association of circulating miRNAs with central biomarkers for AD and their potential utility as blood-based molecular biomarkers for AD. Using PCA, we identified one PC that showed significant associations with AD, CSF p-tau levels, hippocampal volume, and both baseline levels and longitudinal changes in cognition. Among the miRNAs that contributed significantly to the PC, miR-423-5p and miR-92a-3p were identified as key miRNAs. Both miRNAs were found to be significantly

downregulated in AD patients compared to CN individuals, and their lower expression levels were associated with central biomarkers of AD, including reduced hippocampal volume and higher global cortical amyloid deposition. Furthermore, lower levels of these miRNAs were correlated with worse cognitive performance and a faster rate of cognitive decline, indicating their potential role not only as diagnostic biomarkers but also as indicators of disease progression.

Accumulating evidence indicates that miRNAs play important roles in AD pathogenesis through the regulation of genes involved in amyloid processing, tau phosphorylation, and neurodegeneration (Wang et al., 2019; Kou et al., 2020; Guévremont et al., 2022). Our findings align with this evidence by demonstrating associations of lower plasma levels of miR-423-5p and miR-92a-3p with higher global cortical amyloid deposition, reduced hippocampal volume, and worse cognitive performance. Moreover, our study showed a significant
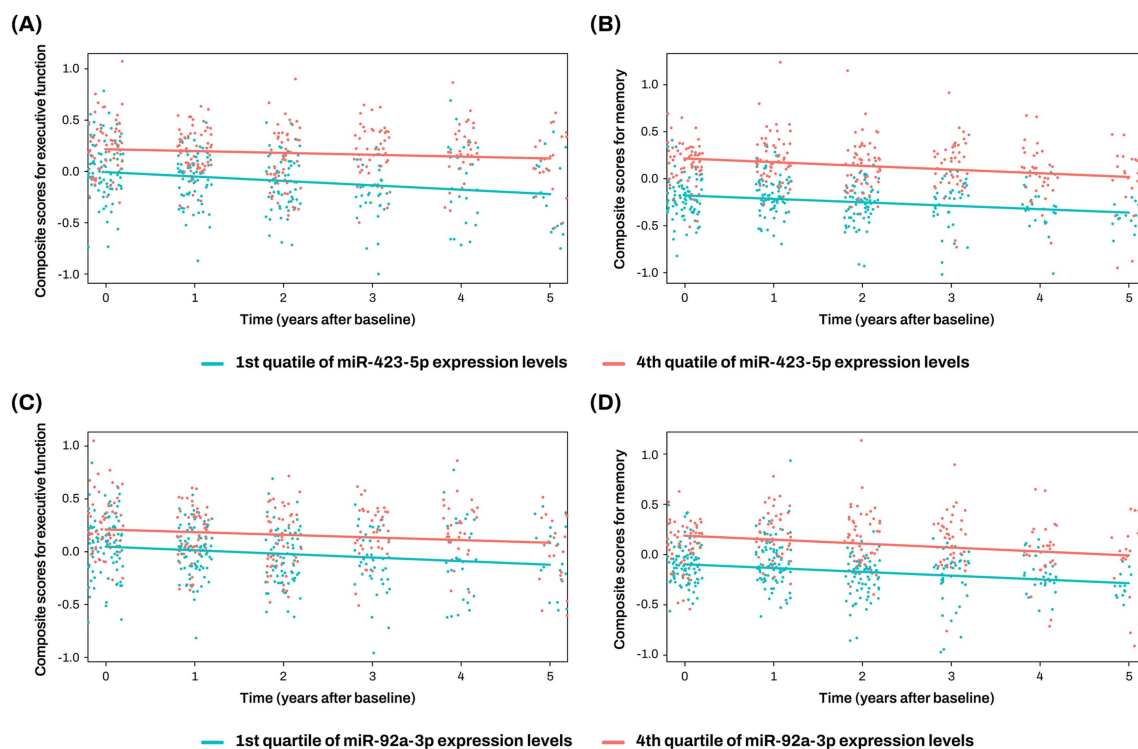
FIGURE 7
Association analysis results of miR-423-5p and miR-92a-3p with longitudinal changes of cognition The x-axis represents years after the initial clinical evaluation, while the y-axis indicates composite scores for executive function **(A,C)** and memory **(B,D)**. The two lines represent the different slopes of changes in composite scores for subjects with 1st quartile (green color) versus 4th quartile (red color) stratified by miR-423-5p **(A,B)** and miR-92a-3p expression levels **(C,D)**. Cognitive scores were standardized as Z-scores. miR, microRNA.
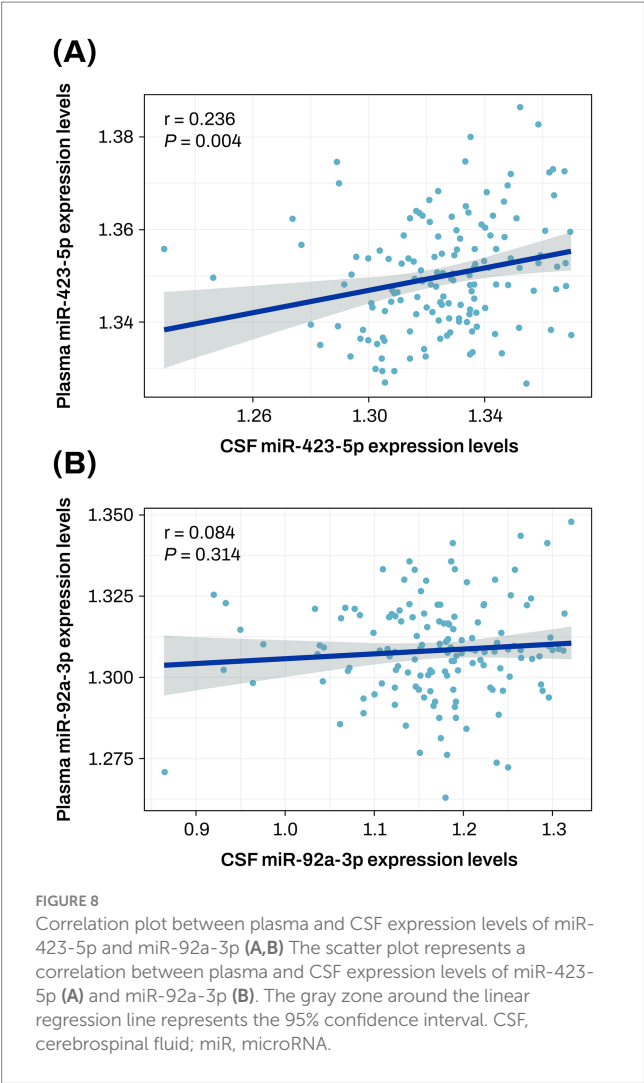
correlation between plasma and CSF expression levels of miR-423-5p, but not for miR-92a-3p. This suggests that miR-423-5p may have potential as a blood-based molecular biomarker reflective of central nervous system changes.

Lower expression levels of miR-423-5p were associated with AD in human cerebral white matter (Wang et al., 2011; Bhattacharyya and Bandyopadhyay, 2013), aligning with findings of our study. Importantly, our study uniquely demonstrates an association between plasma miR-423-5p levels and AD and cognitive function, which has not been previously reported. Furthermore, overexpression of miR-423-5p has been found to enhance cell proliferation, migration, and angiogenesis, and to reduce apoptosis in vivo (Li S. et al., 2017). Lower expression levels of plasma miR-92a-3p have been associated with AD (Peña-Bautista et al., 2022; Piscopo et al., 2023), supporting the findings of our study. Higher expression levels of plasma miR-92a-3p were also found to be significantly associated with better cognitive function (Yaqub et al., 2023; Melas et al., 2024), reinforcing the results of our study. Notably, miR-92a-3p is involved in maintaining blood–brain barrier integrity by regulating tight junctions and endothelial cell function, often compromised in AD (Lu et al., 2021). Additionally, miR-92a plays a critical role in regulating Aβ clearance, accumulation of tau protein, synaptic and gamma-aminobutyric acid-ergic dysfunction in AD (Li X. et al., 2017; Siedlecki-Wullich et al., 2019; Peña-Bautista et al., 2022). Overexpression of miR-92a-3p, one of the miRNAs identified to interact with microtubule-associated protein tau mRNAs, significantly reduced tau protein levels in neuroblastoma cell lines (Piscopo et al.,

2023). We observed significant effect heterogeneity between males and females for the key miRNAs, miR-423-5p and miR-92a-3p, indicating that sex may influence miRNA-related hippocampal atrophy. Our results demonstrate the importance of stratified analyses in uncovering AD-related neurodegeneration that appear to be male-specific.

Pathway enrichment analyses conducted in this study provided insights into the significant biological processes that may be influenced by the target genes of the two AD-associated key miRNAs. Notably, dysregulation in cell migration, proliferation, and differentiation plays a significant role in both AD and Parkinson's disease, underscoring the importance of these pathways in neurodegeneration (Awuson-David et al., 2023). Furthermore, pathways such as protein phosphorylation, including peptidyl-serine and peptidyl-threonine phosphorylation, are critical, as hyperphosphorylation of tau at these residues contributes to its aggregation into NFTs, a hallmark of AD pathology (Wegmann et al., 2021). Lastly, a deficiency in phosphatidylinositol-3-phosphate was identified as a contributing factor to AD pathogenesis by disrupting amyloid precursor protein trafficking and processing (Morel et al., 2013).

The mediation analysis of our study suggests potential roles of miR-423-5p and miR-92a-3p in AD and cognitive function. Specifically, miR-423-5p had both direct and indirect effects on AD through global cortical amyloid deposition and hippocampal volume, while miR-92a-3p did not demonstrate any significant indirect effects. These findings underscore the potential role of miR-423-5p in modulating brain Aβ deposition and neurodegeneration, suggesting its involvement in the molecular mechanisms underlying AD. The lack

FIGURE 8
Correlation plot between plasma and CSF expression levels of miR-423-5p and miR-92a-3p **(A,B)** The scatter plot represents a correlation between plasma and CSF expression levels of miR-423-5p **(A)** and miR-92a-3p **(B)**. The gray zone around the linear regression line represents the 95% confidence interval. CSF, cerebrospinal fluid; miR, microRNA.

of significant mediation effects for miR-92a-3p suggests that its contribution to AD might involve alternative pathways or mechanisms not addressed in our analysis, which requires further exploration to fully understand its role.

The machine learning analysis for differentiating AD patients from CN individuals demonstrated that incorporating miR-423-5p and miR-92a-3p improved the classification performance of demographic information and *APOE* ε4 carrier status for AD classification from the mean AUC value of 0.708 to that of 0.757. This enhancement underscores the potential of miR-423-5p and miR-92a-3p as blood-based molecular biomarkers for AD diagnosis. Integrating these miRNA expression data with demographic information could pave the way for personalized medicine by supporting the development of strategies that account for individual differences in miRNA expression. The clinical relevance of miRNAs extends beyond their role as diagnostic biomarkers, as they are involved in the regulation of molecular pathways implicated in AD pathogenesis. This mechanistic involvement has led to growing interest in miRNA-based therapeutic strategies, including the use of synthetic miRNA mimics and anti-miRNA oligonucleotides aimed at modulating multiple gene expressions and disrupting pathological pathways (Miya Shaik et al., 2018; Bhatnagar et al., 2023).

TABLE 2 Gene ontology analysis of target genes of miR-423-5p and miR-92a-3p.

Biological process	Number of genes from study data/ Number of genes in the pathway (Population Hits)	Fold enrichment	*p* value[a]
Positive regulation of transcription from RNA polymerase II promoter	98/1232	2.088	<0.001
Negative regulation of transcription from RNA polymerase II promoter	78/1016	2.015	<0.001
Brain development	31/264	3.083	<0.001
Protein phosphorylation	40/444	2.365	<0.001
Intracellular signal transduction	41/462	2.330	<0.001
Negative regulation of transcription, DNA-templated	48/591	2.132	<0.001
Peptidyl-serine phosphorylation	23/184	3.282	<0.001
Nervous system development	37/425	2.285	0.002
Neuron migration	17/124	3.599	0.006
Memory	14/89	4.130	0.010
Palate development	12/66	4.773	0.012
Negative regulation of cytoplasmic translation	6/12	13.126	0.017
Ventricular septum morphogenesis	9/37	6.386	0.020
Cell migration	26/278	2.455	0.022
Peptidyl-threonine phosphorylation	12/72	4.375	0.027
Positive regulation of transcription, DNA-templated	50/728	1.803	0.027
Regulation of transcription from RNA polymerase II promoter	97/1736	1.467	0.039
Phosphatidylinositol-3-phosphate biosynthetic process	7/22	8.353	0.044
Cellular response to amino acid stimulus	11/64	4.512	0.047

[a]Adjusted P value for Bonferroni correction. AD, Alzheimer's dementia; miRNAs, microRNAs; mRNA, messenger RNAs.
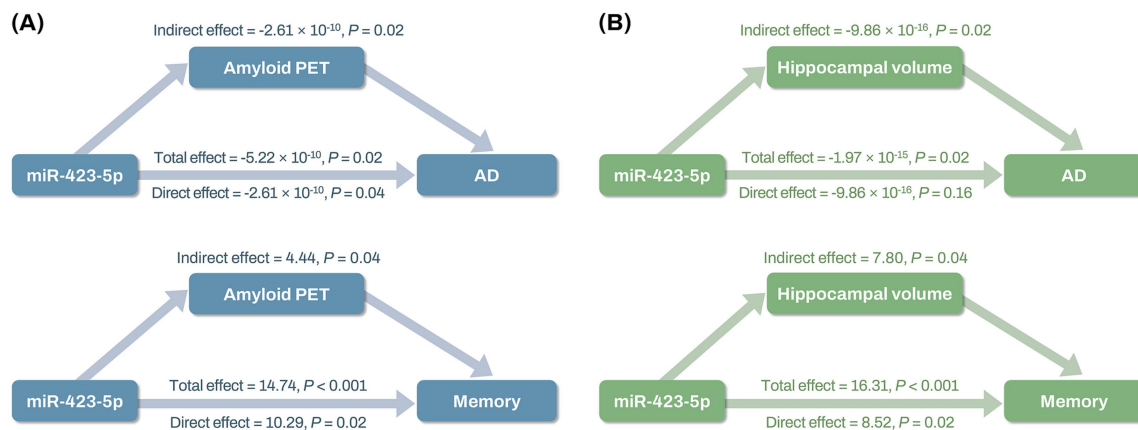
FIGURE 9
Mediation analysis results of miR-423-5p on AD diagnosis and composite scores for memory through global cortical amyloid deposition and hippocampal volume **(A,B)** Mediation analysis shows total, direct, and indirect effects of miR-423-5p expression levels on AD and composite scores for memory through global cortical amyloid deposition **(A)**, and hippocampal volume **(B)**. Hippocampal volume was measured in cubic millimeters (mm^3). Cognitive scores were standardized as Z-scores. AD, Alzheimer's disease; miR, microRNA; PET, positron emission tomography; SUVR, standard uptake value ratio.
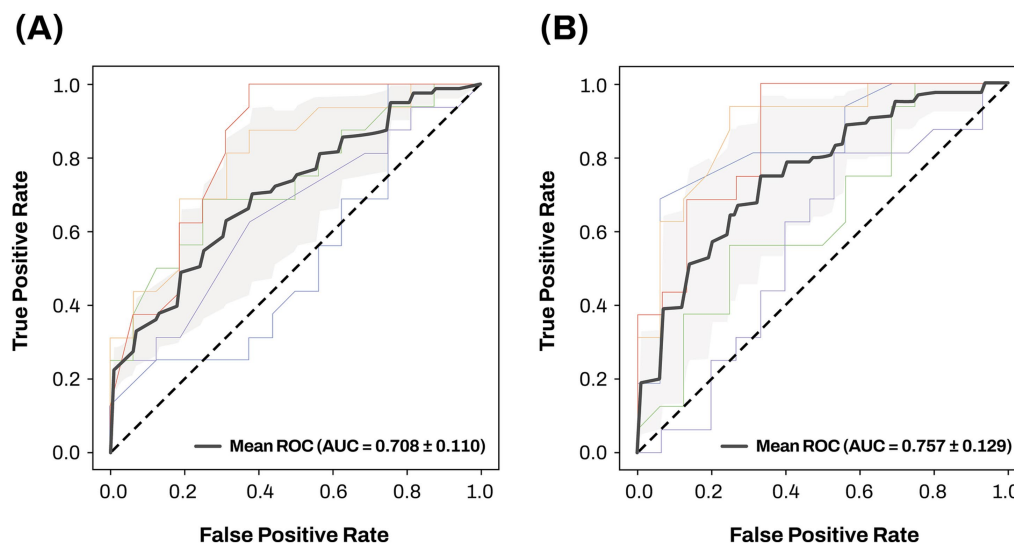
FIGURE 10
The ROC curves and mean AUC of machine learning approach Sensitivity is on the y-axis and 1-specificity is on the x-axis. 5-fold cross validation was used to investigate and compare the classification performance of two different classification models for differentiating AD from CN. The gray zone around the mean ROC curve represents $\pm$ 1 standard deviation. Two different classification models were evaluated using the following training features: **(A)** age, sex, and *APOE ε4* carrier status; **(B)** age, sex, *APOE ε4* carrier status, miR-423-5p, and miR-92a-3p. AD, Alzheimer's disease; *APOE*, apolipoprotein E; AUC, area under the curve; CN, cognitively normal; miRNAs, microRNAs, ROC, receiver operating characteristic.

While this study provides a comprehensive analysis of circulating miRNA expression data with central A/T/N biomarkers and cognitive function within a well-characterized cohort, several limitations need to be addressed in future studies. The modest sample size and lack of external datasets may restrict generalizability, underscoring the need for replication in future large-scale studies. This limitation also affects the clinical applicability of our miRNA-based diagnostic model, which demonstrated the modest classification performance. Moreover,

information on comorbid conditions and medication use was not available in the ADNI dataset, limiting our ability to adjust for these potential confounders. Future longitudinal studies incorporating repeated miRNA measurements will be essential to elucidate the temporal dynamics underlying the observed associations and to establish causality through mediation. Finally, functional studies are crucial to unravel the specific roles of miR-423-5p and miR-92a-3p in AD pathogenesis and to validate their potential as therapeutic targets.

5 Conclusion

In conclusion, this study shows associations of circulating miRNAs (miR-423-5p and miR-92a-3p) with central AD biomarkers and disease progression as well as the improvement in the accuracy of AD classification, shedding light on their potential as blood-based molecular biomarkers for AD. Further investigations are warranted to validate our findings and clarify the underlying mechanisms.

Data availability statement

Publicly available datasets were analyzed in this study. This data can be found at: The ADNI cohort data will be freely available at the ADNI LONI database (http://adni.loni.usc.edu).

Ethics statement

The studies involving humans were approved by the ADNI obtained ethics approvals from all sites collecting data in accordance with the standards of the local ethics committee and Institutional Review Board boards. The studies were conducted in accordance with the local legislation and institutional requirements. Written informed consent for participation in this study was provided by the participants' legal guardians/next of kin.

Author contributions

S-WH: Writing – review & editing, Formal analysis, Software, Methodology, Project administration, Writing – original draft, Data curation, Visualization, Resources, Conceptualization, Validation, Investigation. YP: Software, Writing – review & editing, Investigation, Conceptualization, Supervision, Funding acquisition, Writing – original draft, Data curation, Validation, Resources, Visualization, Formal analysis, Project administration, Methodology. J-MP: Writing – original draft, Writing – review & editing. PB: Writing – original draft, Writing – review & editing. SK: Writing – original draft, Writing – review & editing. AS: Writing – review & editing, Writing – original draft. KN: Validation, Project administration, Methodology, Formal analysis, Supervision, Data curation, Software, Writing – original draft, Visualization, Conceptualization, Resources, Investigation, Writing – review & editing.

Funding

Acknowledgments

Conflict of interest

The authors declare that the research was conducted in the absence of any commercial or financial relationships that could be construed as a potential conflict of interest.

The handling editor AT declared a past collaboration with the authors PB, AS and KN.

Generative AI statement

The authors declare that no Gen AI was used in the creation of this manuscript.

Publisher's note

All claims expressed in this article are solely those of the authors and do not necessarily represent those of their affiliated organizations, or those of the publisher, the editors and the reviewers. Any product that may be evaluated in this article, or claim that may be made by its manufacturer, is not guaranteed or endorsed by the publisher.

Supplementary material

The Supplementary material for this article can be found online at: https://www.frontiersin.org/articles/10.3389/fnagi.2025.1637368/full#supplementary-material

References

Abdalla, M., Lam, B., Simkin, M., Rghei, N., and Haj-Ahmad, Y. (2011). *Effect of RNA isolation method on microRNA quantity and quality in plasma: A comparative study.* Norgen Biotek corporation application note 49: RNA sample preparation.

Aisen, P. S., Petersen, R. C., Donohue, M. C., Gamst, A., Raman, R., Thomas, R. G., et al. (2010). Clinical Core of the Alzheimer's disease neuroimaging Initiative: progress and plans. *Alzheimers Dement.* 6, 239–246. doi: 10.1016/j.jalz.2010.03.006

Aisen, P. S., Petersen, R. C., Donohue, M., and Weiner, M. W.Alzheimer's Disease Neuroimaging Initiative (2015). Alzheimer's disease neuroimaging initiative 2 clinical core: progress and plans. *Alzheimers Dement.* 11, 734–739. doi: 10.1016/j.jalz.2015.05.005

Arnold, M., Nho, K., Kueider-Paisley, A., Massaro, T., Huynh, K., Brauner, B., et al. (2020). Sex and APOE ε4 genotype modify the Alzheimer's disease serum metabolome. *Nat. Commun.* 11:1148. doi: 10.1038/s41467-020-14959-w

Ashburner, M., Ball, C. A., Blake, J. A., Botstein, D., Butler, H., Cherry, J. M., et al. (2000). Gene ontology: tool for the unification of biology. *Nat. Genet.* 25, 25–29. doi: 10.1038/75556

Awuson-David, B., Williams, A. C., Wright, B., Hill, L. J., and Di Pietro, V. (2023). Common microRNA regulated pathways in Alzheimer's and Parkinson's disease. *Front. Neurosci.* 17:1228927. doi: 10.3389/fnins.2023.1228927

Bartel, D. P. (2004). Micrornas: genomics, biogenesis, mechanism, and function. *Cell* 116, 281–297. doi: 10.1016/s0092-8674(04)00045-5

Benjamini, Y., and Hochberg, Y. (1995). Controlling the false discovery rate: a practical and powerful approach to multiple testing. *J. R. Stat. Soc. Ser. B Stat Methodol.* 57, 289–300. doi: 10.1111/j.2517-6161.1995.tb02031.x

Bhatnagar, D., Ladhe, S., and Kumar, D. (2023). Discerning the prospects of miRNAs as a multi-target therapeutic and diagnostic for Alzheimer's disease. *Mol. Neurobiol.* 60, 5954–5974. doi: 10.1007/s12035-023-03446-0

Bhattacharyya, M., and Bandyopadhyay, S. (2013). Studying the differential co-expression of microRNAs reveals significant role of white matter in early Alzheimer's progression. *Mol. BioSyst.* 9, 457–466. doi: 10.1039/c2mb25434d

Bittner, T., Zetterberg, H., Teunissen, C. E., Ostlund, R. E. Jr., Militello, M., Andreasson, U., et al. (2016). Technical performance of a novel, fully automated electrochemiluminescence immunoassay for the quantitation of β-amyloid (1–42) in human cerebrospinal fluid. *Alzheimers Dement.* 12, 517–526. doi: 10.1016/j.jalz.2015.09.009

Dunn, O. J. (1961). Multiple comparisons among means. *J. Am. Stat. Assoc.* 56, 52–64. doi: 10.1080/01621459.1961.10482090

Fabrigar, L. R., Wegener, D. T., MacCallum, R. C., and Strahan, E. J. (1999). Evaluating the use of exploratory factor analysis in psychological research. *Psychol. Methods* 4, 272–299. doi: 10.1037/1082-989X.4.3.272

Folstein, M. F., Folstein, S. E., and McHugh, P. R. (1975). "Mini-mental state": a practical method for grading the cognitive state of patients for the clinician. *J. Psychiatr. Res.* 12, 189–198. doi: 10.1016/0022-3956(75)90026-6

Guévremont, D., Tsui, H., Knight, R., Fowler, C. J., Masters, C. L., Martins, R. N., et al. (2022). Plasma microRNA vary in association with the progression of Alzheimer's disease. *Alzheimers Dement (Amst)* 14:e12251. doi: 10.1002/dad2.12251

Hampel, H., Frank, R., Broich, K., Teipel, S. J., Katz, R. G., Hardy, J., et al. (2010). Biomarkers for Alzheimer's disease: academic, industry and regulatory perspectives. *Nat. Rev. Drug Discov.* 9, 560–574. doi: 10.1038/nrd3115

Hampel, H., O'Bryant, S. E., Molinuevo, J. L., Zetterberg, H., Masters, C. L., Lista, S., et al. (2018). Blood-based biomarkers for Alzheimer's disease: mapping the road to the clinic. *Nat. Rev. Neurol.* 14, 639–652. doi: 10.1038/s41582-018-0079-7

Hansson, O., Seibyl, J., Stomrud, E., Zetterberg, H., Trojanowski, J. Q., Bittner, T., et al. (2018). CSF biomarkers of Alzheimer's disease concord with amyloid-β PET and predict clinical progression: a study of fully automated immunoassays in BioFINDER and ADNI cohorts. *Alzheimers Dement.* 14, 1470–1481. doi: 10.1016/j.jalz.2018.01.010

Hayes, A. F. (2009). Beyond baron and Kenny: statistical mediation analysis in the new millennium. *Commun. Monogr.* 76, 408–420. doi: 10.1080/03637750903310360

Higgins, J. P., and Thompson, S. G. (2002). Quantifying heterogeneity in a meta-analysis. *Stat. Med.* 21, 1539–1558. doi: 10.1002/sim.1186

Huang, D. W., Sherman, B. T., and Lempicki, R. A. (2009). Systematic and integrative analysis of large gene lists using DAVID bioinformatics resources. *Nat. Protoc.* 4, 44–57. doi: 10.1038/nprot.2008.211

Jack, C. R., Andrews, J. S., Beach, T. G., Buracchio, T., Dunn, B., Graf, A., et al. (2024). Revised criteria for diagnosis and staging of Alzheimer's disease: Alzheimer's Association workgroup. *Alzheimers Dement.* 20, 5143–5169. doi: 10.1002/alz.13859

Jack, C. R., Bernstein, M. A., Borowski, B. J., Gunter, J. L., Fox, N. C., Thompson, P. M., et al. (2010). Update on the magnetic resonance imaging core of the Alzheimer's disease neuroimaging initiative. *Alzheimers Dement.* 6, 212–220. doi: 10.1016/j.jalz.2010.03.004

Jack, C. R., Bernstein, M. A., Fox, N. C., Thompson, P., Alexander, G., Harvey, D., et al. (2008). The Alzheimer's disease neuroimaging initiative (ADNI): MRI methods. *J. Magn. Reson. Imaging* 27, 685–691. doi: 10.1002/jmri.21049

Jagust, W. J., Bandy, D., Chen, K., Foster, N. L., Landau, S. M., Mathis, C. A., et al. (2010). The Alzheimer's disease neuroimaging Initiative positron emission tomography core. *Alzheimers Dement.* 6, 221–229. doi: 10.1016/j.jalz.2010.03.003

Jagust, W. J., Landau, S. M., Koeppe, R. A., Reiman, E. M., Chen, K., Mathis, C. A., et al. (2015). The Alzheimer's disease neuroimaging initiative 2 PET core: 2015. *Alzheimers Dement.* 11, 757–771. doi: 10.1016/j.jalz.2015.05.001

Jolliffe, I. T. (2002). Principal component analysis for special types of data. New York: Springer.

Jolliffe, I. T., and Cadima, J. (2016). Principal component analysis: a review and recent developments. *Philos. Trans. A. Math. Phys. Eng. Sci.* 374:20150202. doi: 10.1098/rsta.2015.0202

Joshi, A. D., Pontecorvo, M. J., Clark, C. M., Carpenter, A. P., Jennings, D. L., Sadowsky, C. H., et al. (2012). Performance characteristics of amyloid PET with florbetapir F 18 in patients with Alzheimer's disease and cognitively normal subjects. *J. Nucl. Med.* 53, 378–384. doi: 10.2967/jnumed.111.090340

Kang, J.-H., Korecka, M., Figurski, M. J., Toledo, J. B., Blennow, K., Zetterberg, H., et al. (2015). The Alzheimer's disease neuroimaging initiative 2 biomarker core: a review of progress and plans. *Alzheimers Dement.* 11, 772–791. doi: 10.1016/j.jalz.2015.05.003

Kou, X., Chen, D., and Chen, N. (2020). The regulation of microRNAs in Alzheimer's disease. *Front. Neurol.* 11:288. doi: 10.3389/fneur.2020.00288

Lewis, B. P., Burge, C. B., and Bartel, D. P. (2005). Conserved seed pairing, often flanked by adenosines, indicates that thousands of human genes are microRNA targets. *Cell* 120, 15–20. doi: 10.1016/j.cell.2004.12.035

Li, X., Wang, Z., Tan, L., Wang, Y., Lu, C., Chen, R., et al. (2017). Correcting miR92a-vGAT-mediated GABAergic dysfunctions rescues human tau-induced anxiety in mice. *Mol. Ther.* 25, 140–152. doi: 10.1016/j.ymthe.2016.10.010

Li, Y., Wu, F.-X., and Ngom, A. (2018). A review on machine learning principles for multi-view biological data integration. *Brief. Bioinform.* 19, 325–340. doi: 10.1093/bib/bbw113

Li, S., Zeng, A., Hu, Q., Yan, W., Liu, Y., and You, Y. (2017). miR-423-5p contributes to a malignant phenotype and temozolomide chemoresistance in glioblastomas. *Neuro-Oncology* 19, 55–65. doi: 10.1093/neuonc/now129

Long, J. M., and Holtzman, D. M. (2019). Alzheimer disease: an update on pathobiology and treatment strategies. *Cell* 179, 312–339. doi: 10.1016/j.cell.2019.09.001

Lu, L., Lu, T., Shen, J., Lv, X., Wei, W., Wang, H., et al. (2021). Alisol A 24-acetate protects against brain microvascular endothelial cells injury through inhibiting miR-92a-3p/tight junctions axis. *Aging (Albany NY)* 13, 15353–15365. doi: 10.18632/aging.203094

Lusardi, T. A., Phillips, J. I., Wiedrick, J. T., Harrington, C. A., Lind, B., Lapidus, J. A., et al. (2016). MicroRNAs in human cerebrospinal fluid as biomarkers for Alzheimer's disease. *J Alzheimer's Dis* 55, 1223–1233. doi: 10.3233/JAD-160835

Melas, K., Talevi, V., Imtiaz, M. A., Etteldorf, R., Estrada, S., Krüger, D. M., et al. (2024). Blood-derived microRNAs are related to cognitive domains in the general population. *Alzheimers Dement.* 20, 7138–7159. doi: 10.1002/alz.14197

Meng, C., Zeleznik, O. A., Thallinger, G. G., Kuster, B., Gholami, A. M., and Culhane, A. C. (2016). Dimension reduction techniques for the integrative analysis of multi-omics data. *Brief. Bioinform.* 17, 628–641. doi: 10.1093/bib/bbv108

Miya Shaik, M., Tamargo, I. A., Abubakar, M. B., Kamal, M. A., Greig, N. H., and Gan, S. H. (2018). The role of microRNAs in Alzheimer's disease and their therapeutic potentials. *Genes (Basel)* 9:174. doi: 10.3390/genes9040174

Mohs, R. C., Knopman, D., Petersen, R. C., Ferris, S. H., Ernesto, C., Grundman, M., et al. (1997). Development of cognitive instruments for use in clinical trials of antidementia drugs: additions to the Alzheimer's disease assessment scale that broaden its scope. *Alzheimer Dis. Assoc. Disord.* 11, 13–21. doi: 10.1097/00002093-199700112-00003

Moldovan, L., Batte, K. E., Trgovcich, J., Wisler, J., Marsh, C. B., and Piper, M. (2014). Methodological challenges in utilizing mi RNA s as circulating biomarkers. *J. Cell. Mol. Med.* 18, 371–390. doi: 10.1111/jcmm.12236

Morel, E., Chamoun, Z., Lasiecka, Z. M., Chan, R. B., Williamson, R. L., Vetanovetz, C., et al. (2013). Phosphatidylinositol-3-phosphate regulates sorting and processing of amyloid precursor protein through the endosomal system. *Nat. Commun.* 4:2250. doi: 10.1038/ncomms3250

Morris, J. C. (1993). The clinical dementia rating (CDR) current version and scoring rules. *Neurology* 43:2412-2412-a.

Morris, J. C., Heyman, A., Mohs, R. C., Hughes, J., van Belle, G., Fillenbaum, G., et al. (1989). The consortium to establish a registry for Alzheimer's disease (CERAD). Part I. Clinical and neuropsychological assessment of Alzheimer's disease. *Neurology* 39, 1159–1165. doi: 10.1212/wnl.39.9.1159

Paternoster, R., Brame, R., Mazerolle, P., and Piquero, A. (1998). Using the correct statistical test for the equality of regression coefficients. *Criminology* 36, 859–866. doi: 10.1111/j.1745-9125.1998.tb01268.x

Peña-Bautista, C., Tarazona-Sánchez, A., Braza-Boils, A., Balaguer, A., Ferré-González, L., Cañada-Martínez, A. J., et al. (2022). Plasma microRNAs as potential

biomarkers in early Alzheimer disease expression. *Sci. Rep.* 12:15589. doi: 10.1038/s41598-022-19862-6

Peres-Neto, P. R., Jackson, D. A., and Somers, K. M. (2005). How many principal components? Stopping rules for determining the number of non-trivial axes revisited. *Comput. Stat. Data Anal.* 49, 974–997. doi: 10.1016/j.csda.2004.06.015

Petersen, R. C., Aisen, P. S., Beckett, L. A., Donohue, M. C., Gamst, A. C., Harvey, D. J., et al. (2010). Alzheimer's disease neuroimaging Initiative (ADNI) clinical characterization. *Neurology* 74, 201–209. doi: 10.1212/WNL.0b013e3181cb3e25

Piscopo, P., Grasso, M., Manzini, V., Zeni, A., Castelluzzo, M., Fontana, F., et al. (2023). Identification of miRNAs regulating MAPT expression and their analysis in plasma of patients with dementia. *Front. Mol. Neurosci.* 16:1127163. doi: 10.3389/fnmol.2023.1127163

Reitan, R. M., and Wolfson, D. (1985). *The Halstead-Reitan neuropsychological test battery: Theory and clinical interpretation.* Tucson: Neuropsychology Press.

Rey, A. (1983). *Rey auditory-verbal learning test.*

Ringnér, M. (2008). What is principal component analysis? *Nat. Biotechnol.* 26, 303–304. doi: 10.1038/nbt0308-303

Sandau, U. S., Duggan, E., Shi, X., Smith, S. J., Huckans, M., Schutzer, W. E., et al. (2020a). Methamphetamine use alters human plasma extracellular vesicles and their microRNA cargo: an exploratory study. *J. Extracell. Vesicles* 10:e12028. doi: 10.1002/jev2.12028

Sandau, U. S., McFarland, T. J., Smith, S. J., Galasko, D. R., Quinn, J. F., and Saugstad, J. A. (2022). Differential effects of APOE genotype on MicroRNA cargo of cerebrospinal fluid extracellular vesicles in females with Alzheimer's disease compared to males. *Front. Cell Dev. Biol.* 10:864022. doi: 10.3389/fcell.2022.864022

Sandau, U. S., Wiedrick, J. T., McFarland, T. J., Galasko, D. R., Fanning, Z., Quinn, J. F., et al. (2024). Analysis of the longitudinal stability of human plasma miRNAs and implications for disease biomarkers. *Sci. Rep.* 14:2148. doi: 10.1038/s41598-024-52681-5

Sandau, U. S., Wiedrick, J. T., Smith, S. J., McFarland, T. J., Lusardi, T. A., Lind, B., et al. (2020b). Performance of validated microRNA biomarkers for Alzheimer's disease in mild cognitive impairment. *J Alzheimer's Dis* 78, 245–263. doi: 10.3233/JAD-200396

Saugstad, J. A., Lusardi, T. A., Van Keuren-Jensen, K. R., Phillips, J. I., Lind, B., Harrington, C. A., et al. (2017). Analysis of extracellular RNA in cerebrospinal fluid. *J Extracell Vesicles* 6:1317577. doi: 10.1080/20013078.2017.1317577

Schindler, S. E., Galasko, D., Pereira, A. C., Rabinovici, G. D., Salloway, S., Suárez-Calvet, M., et al. (2024). Acceptable performance of blood biomarker tests of amyloid pathology—recommendations from the global CEO Initiative on Alzheimer's disease. *Nat. Rev. Neurol.* 20, 426–439. doi: 10.1038/s41582-024-00977-5

Scientific, T. F. (2017). *Qubit 4 fluorometer user guide.*

Siedlecki-Wullich, D., Català-Solsona, J., Fábregas, C., Hernández, I., Clarimon, J., Lleó, A., et al. (2019). Altered microRNAs related to synaptic function as potential plasma biomarkers for Alzheimer's disease. *Alzheimer's Res Ther* 11, 1–11. doi: 10.1186/s13195-019-0501-4

TaqMan, C. (2011). *TaqMan® small RNA assays.*

Tingley, D., Yamamoto, T., Hirose, K., Keele, L., and Imai, K. (2014). Mediation: R package for causal mediation analysis. *J. Stat. Softw.* 59:5. doi: 10.18637/jss.v059.i05

Turchinovich, A., Weiz, L., Langheinz, A., and Burwinkel, B. (2011). Characterization of extracellular circulating microRNA. *Nucleic Acids Res.* 39, 7223–7233. doi: 10.1093/nar/gkr254

Urbanowicz, R., Zhang, R., Cui, Y., and Suri, P. (2023). STREAMLINE: a simple, transparent, end-to-end automated machine learning pipeline facilitating data analysis and algorithm comparison, Genetic Programming Theory and Practice XIX. Berlin: Springer, 201–231.

Wang, W.-X., Huang, Q., Hu, Y., Stromberg, A. J., and Nelson, P. T. (2011). Patterns of microRNA expression in normal and early Alzheimer's disease human temporal cortex: white matter versus gray matter. *Acta Neuropathol.* 121, 193–205. doi: 10.1007/s00401-010-0756-0

Wang, M., Qin, L., and Tang, B. (2019). Micrornas in Alzheimer's disease. *Front. Genet.* 10:153. doi: 10.3389/fgene.2019.00153

Weber, J. A., Baxter, D. H., Zhang, S., Huang, D. Y., How Huang, K., Jen Lee, M., et al. (2010). The microRNA spectrum in 12 body fluids. *Clin. Chem.* 56, 1733–1741. doi: 10.1373/clinchem.2010.147405

Wechsler, D. (1987). WMS-R: Wechsler memory scale-revised. San Antonio, TX: Psychological Corporation.

Wechsler, D., and De Lemos, M. M. (1981). Wechsler adult intelligence scale-revised. New York: Psychological Corporation.

Wegmann, S., Biernat, J., and Mandelkow, E. (2021). A current view on tau protein phosphorylation in Alzheimer's disease. *Curr. Opin. Neurobiol.* 69, 131–138. doi: 10.1016/j.conb.2021.03.003

Weiner, M. W., Veitch, D. P., Aisen, P. S., Beckett, L. A., Cairns, N. J., Green, R. C., et al. (2017). The Alzheimer's disease neuroimaging Initiative 3: continued innovation for clinical trial improvement. *Alzheimers Dement.* 13, 561–571. doi: 10.1016/j.jalz.2016.10.006

Wiedrick, J. T., Phillips, J. I., Lusardi, T. A., McFarland, T. J., Lind, B., Sandau, U. S., et al. (2019). Validation of microRNA biomarkers for Alzheimer's disease in human cerebrospinal fluid. *J Alzheimer's Dis* 67, 875–891. doi: 10.3233/JAD-180539

Winter, J., Jung, S., Keller, S., Gregory, R. I., and Diederichs, S. (2009). Many roads to maturity: microRNA biogenesis pathways and their regulation. *Nat. Cell Biol.* 11, 228–234. doi: 10.1038/ncb0309-228

Wong, N., and Wang, X. (2015). miRDB: an online resource for microRNA target prediction and functional annotations. *Nucleic Acids Res.* 43, D146–D152. doi: 10.1093/nar/gku1104

Yaqub, A., Mens, M. M., Klap, J. M., Weverling, G. J., Klatser, P., Brakenhoff, J. P., et al. (2023). Genome-wide profiling of circulatory microRNAs associated with cognition and dementia. *Alzheimers Dement.* 19, 1194–1203. doi: 10.1002/alz.12752